CD146/Soluble CD146 Pathway Is a Novel Biomarker of Angiogenesis and Inflammation in Proliferative Diabetic Retinopathy

Ahmed M. Abu El-Asrar,[1,2] Mohd Imtiaz Nawaz,[1] Ajmal Ahmad,[1] Mohammad Mairaj Siddiquei,[1] Eef Allegaert,[3,4] Priscilla W. Gikandi,[1] Gert De Hertogh,[3,4] and Ghislain Opdenakker[4,5]

[1]Department of Ophthalmology, College of Medicine and Medical City, King Saud University, Riyadh, Saudi Arabia
[2]Dr. Nasser Al-Rashid Research Chair in Ophthalmology, College of Medicine, King Saud University, Riyadh, Saudi Arabia
[3]Laboratory of Histochemistry and Cytochemistry, University of Leuven (KU Leuven), Leuven, Belgium
[4]University Hospitals, UZ Gasthuisberg, Leuven, Belgium
[5]Department of Microbiology and Immunology and Transplantation, Rega Institute for Medical Research, University of Leuven (KU Leuven), Leuven, Belgium

Correspondence: Ahmed M. Abu El-Asrar, Department of Ophthalmology King Abdulaziz University Hospital Old Airport Road, P.O. Box 245, Riyadh 11411, Saudi Arabia;
abuelasrar@yahoo.com;
abuasrar@KSU.edu.sa.

AMA and MIN are joint first authors.

Received: November 5, 2020
Accepted: April 18, 2021
Published: July 22, 2021

Citation: Abu El-Asrar AM, Nawaz MI, Ahmad A, et al. CD146/soluble CD146 pathway is a novel biomarker of angiogenesis and inflammation in proliferative diabetic retinopathy. *Invest Ophthalmol Vis Sci.* 2021;62(9):32.
https://doi.org/10.1167/iovs.62.9.32

Purpose. Inflammation, angiogenesis and fibrosis are pathological hallmarks of proliferative diabetic retinopathy (PDR). The CD146/sCD146 pathway displays proinflammatory and proangiogenic properties. We investigated the role of this pathway in the pathophysiology of PDR.

Methods. Vitreous samples from 41 PDR and 27 nondiabetic patients, epiretinal fibrovascular membranes from 18 PDR patients, rat retinas, human retinal microvascular endothelial cells (HRMECs) and human retinal Müller glial cells were studied by ELISA, Western blot analysis, immunohistochemistry and immunofluorescence microscopy analysis. Blood-retinal barrier breakdown was assessed with fluorescein isothiocyanate-conjugated dextran.

Results. sCD146 and VEGF levels were significantly higher in vitreous samples from PDR patients than in nondiabetic patients. In epiretinal membranes, immunohistochemical analysis revealed CD146 expression in leukocytes, vascular endothelial cells and myofibroblasts. Significant positive correlations were detected between numbers of blood vessels expressing CD31, reflecting angiogenic activity of PDR, and numbers of blood vessels and stromal cells expressing CD146. Western blot analysis showed significant increase of CD146 in diabetic rat retinas. sCD146 induced upregulation of phospho-ERK1/2, NF-κB , VEGF and MMP-9 in Müller cells. The hypoxia mimetic agent cobalt chloride, VEGF and TNF-α induced upregulation of sCD146 in HRMECs. The MMP inhibitor ONO-4817 attenuated TNF-α-induced upregulation of sCD146 in HRMECs. Intravitreal administration of sCD146 in normal rats significantly increased retinal vascular permeability and induced significant upregulation of phospho-ERK1/2, intercellular adhesion molecule-1 and VEGF in the retina. sCD146 induced migration of HRMECs.

Conclusions. These results suggest that the CD146/sCD146 pathway is involved in the initiation and progression of PDR.

Keywords: proliferative diabetic retinopathy, CD146, Müller cells, inflammation, angiogenesis

Ischemia-induced retinal angiogenesis, the formation of new blood vessels from preexisting microvasculature, and expansion of extracellular matrix are crucial processes during initiation and progression of proliferative diabetic retinopathy (PDR). The outgrowth of fibrovascular epiretinal membranes at the vitreoretinal interface often leads to catastrophic visual loss due to vitreous hemorrhage and/or traction retinal detachment. In addition to angiogenesis and fibrosis, recruitment of leukocytes and inflammatory conditions are present in the ocular microenvironment of patients with PDR.[1–6] Leukocytes in the surgically excised fibrovascular epiretinal membranes from patients with PDR have been shown to supply proinflammatory and proangiogenic factors.[1–6] These observations indicate that leukocytes play an important pathophysiologic role in PDR. The link between chronic inflammation and angiogenesis has recently been reinforced in several studies.[7,8] These findings suggest that the relationship between inflammation and angiogenesis is critical for initiation and progression of PDR.

Several angiogenic and inflammatory factors are upregulated in the ocular microenvironment of patients with PDR.[1–6] Among these factors, the proangiogenic factor vascular endothelial growth factor (VEGF), released in response to hypoxia, is a key player of angiogenesis and vascular leakage.[9] VEGF exerts its angiogenic effects by binding to its transmembrane tyrosine kinase receptor VEGFR-2 which is expressed on vascular endothelial cells and is the major receptor for pathological angiogenesis as well as microvascular permeability.[10] Targeting the VEGF/VEGFR-2 pathway has emerged as an important therapeutic approach to arrest progression of angiogenesis in patients with PDR.[11] However, these approaches often lead to transient responses because angiogenesis is regulated by multiple pathways and when the activity of one pathway, such as VEGF/VEGFR-2 is suppressed, the expression of other compensatory angiogenic pathways may appear and contribute to limit the efficacy of anti-VEGF treatment.[12] Therefore, the identification of those compensatory signaling pathways linking hypoxia to angiogenesis in the ocular microenvironment of patients with PDR is essential to design novel therapies aiming at inhibiting simultaneously different angiogenic pathways.

Cluster of differentiation 146 (CD146) also known as melanoma cell adhesion molecule (MCAM) is a cell adhesion molecule belonging to the immunoglobulin superfamily. It was originally described as a marker of tumor growth and metastasis in human melanoma. Since this initial discovery, CD146 was found to be upregulated in several types of cancer and its overexpression is associated with poor prognosis. Therefore, CD146 was identified as a valuable prognostic biomarker in cancer.[13,14] Thereafter, CD146 was also found to be highly expressed in the endothelium, and has been described as a component of the endothelial junctions. It has also been identified on smooth muscle cells, pericytes and some immune cells.[14] In addition to the membrane-anchored forms of CD146, a soluble form of CD146 (sCD146) is identified which is generated by the proteolytic cleavage of the membrane form as the result of matrix metalloproteinase (MMP)-dependent shedding.[15] CD146 was identified as a coreceptor for VEGFR-2 in the endothelium[16] and mediates VEGF-induced *in vitro* and *in vivo* angiogenesis.[16–18] Targeting CD146 was effective to inhibit *in vitro* and *in vivo* angiogenesis.[17–19] In addition, sCD146 was shown to display angiogenic properties *in vitro* and *in vivo*.[20,21]

In addition to its role in angiogenesis, CD146 displays proinflammatory properties. sCD146 was found to promote *in vitro* endothelial permeability[22] and leukocyte transmigration[23] in a surrogate model of the blood brain barrier. In an *in vitro* transmigration model, both membrane and soluble forms of CD146 were demonstrated to be involved in monocyte transmigration through the endothelial monolayer.[24] Endothelial CD146 is actively involved in the transmigration of lymphocytes across the blood-brain barrier and promotes the formation of central nervous system lesions in experimental autoimmune encephalomyelitis, an animal model of multiple sclerosis. Selectively deleting CD146 expression in vascular endothelial cells or blocking endothelial CD146 with a specific antibody cause significant reductions in the infiltration of pathogenic lymphocytes into the central nervous system and decrease neuroinflammation.[25]

Given the key roles of CD146 in the regulation of angiogenesis, vascular permeability and leukocyte transmigration, we hypothesized that the CD146/sCD146 pathway may be involved in the pathogenesis of PDR.

Materials and Methods

Patient Samples

The study was conducted according to the tenets of the Declaration of Helsinki. All the patients were candidates for vitrectomy as a surgical procedure. All patients signed a preoperative informed written consent and approved the use of the excised epiretinal membranes and vitreous fluid for further analysis and clinical research. The study design and the protocol were approved by the Research Centre and Institutional Review Board of the College of Medicine, King Saud University.

Undiluted vitreous fluid samples (0.3–0.6 ml) were obtained from 41 patients with PDR during pars plana vitrectomy, for the treatment of tractional retinal detachment, and/or nonclearing vitreous hemorrhage and processed as described previously.[1–6] We compared the samples from diabetic patients with those of a clinical control cohort. The control group consisted of 27 patients who had undergone vitrectomy for the treatment of rhegmatogenous retinal detachment with no proliferative vitreoretinopathy (PVR). Control subjects were clinically checked to be free from diabetes or other systemic disease. Vitreous samples were collected undiluted by manual suction into a syringe through the aspiration line of vitrectomy, before opening the infusion line. The samples were centrifuged (700 X g for 10 min, 4°C) and the supernatants were aliquoted and frozen at −80°C until assay. Epiretinal fibrovascular membranes were obtained from 18 patients with PDR during pars plana vitrectomy for the repair of tractional retinal detachment. The severity of retinal neovascular activity was graded clinically at the time of vitrectomy using previously published criteria.[26] Neovascularization was considered active if perfused new vessels were visible on the retina or optic disc. Neovascularization was considered inactive (involuted) if only nonvascularized, white fibrotic epiretinal membranes were present. For comparison, epiretinal fibrocellular membranes were obtained from 10 patients without diabetes undergoing vitreoretinal surgery for the treatment of retinal detachment complicated by PVR. All the epiretinal membrane samples were processed as previously described.[1–6] Membranes were fixed for 2h in 10% formalin solution and embedded in paraffin.

Enzyme-Linked Immunosorbent Assays of Human Vitreous Fluid and Culture Medium

Enzyme-linked immunosorbent assay (ELISA) kits for human sCD146 (Cat No DY932-05) and human VEGF (Cat No SVE00) were purchased from R&D Systems. The ELISA kit for human MMP-9 (Cat No ab100610) was purchased from Abcam (Cambridge, UK). Levels of human sCD146 and VEGF in vitreous fluid and sCD146, VEGF and MMP-9 in culture medium were determined with the aforementioned ELISA kits according to the manufacturer's instructions. The minimum detection limits for VEGF and MMP-9 ELISA kits were 9 pg/ml and 10pg/ml, respectively.

Immunohistochemical Staining of Human Epiretinal Membranes and Quantitations

For CD31 and α-SMA detection, antigen retrieval was performed by boiling the sections in citrate based buffer [pH 5.9–6.1] [BOND Epitope Retrieval Solution 1; Leica]

for 10 minutes. For CD45 and CD146 detection, antigen retrieval was performed by boiling the sections in Tris/EDTA buffer [pH 9] [BOND Epitope Retrieval Solution 2; Leica] for 20 minutes. Subsequently, the sections were incubated for 60 minutes with mouse monoclonal anti-CD31 (ready-to-use; clone JC70A; Dako, Glostrup, Denmark), mouse monoclonal anti-CD45 (ready-to-use; clones 2B11+PD7/26; Dako), mouse monoclonal antibody against α-SMA (ready-to-use: clone 1A4; Dako) and rabbit polyclonal anti-CD146 antibody (1:50; ab 203118, Abcam). Optimal working conditions for the antibodies were determined in pilot experiments on human kidney, tonsil and liver sections. The sections were then incubated for 20 minutes with an IgG, conjugated with alkaline phosphatase. The reaction product was visualized by incubation for 15 minutes with the Fast Red chromogen, resulting in bright-red immunoreactive sites. The slides were then faintly counterstained with Mayer's hematoxylin [BOND Polymer Refine Red Detection Kit; Leica].

To identify the phenotype of cells expressing CD146, sequential double immunohistochemistry was performed. The sections were incubated with the first primary antibody (anti-CD45) and subsequently treated with peroxidase-conjugated secondary antibody to define the leukocytes. The resulting immune complexes were visualized by enzymatic reaction of the 3, 3'-diaminobenzidine tetrahydrochloride substrate. Incubation of the second primary antibody (anti-CD146) was followed by treatment with alkaline phosphatase-conjugated secondary antibody and Fast Red reactions. No counterstain was applied. In negative controls, the incubation step with primary antibodies was omitted from the staining protocol. Instead, the ready-to-use DAKO Real antibody Diluent (Agilent Technologies Product Code 52022) was applied.

The level of vascularization in epiretinal membranes was determined by immunodetection of the vascular endothelium marker CD31. Quantification of CD31-positive vessels in tumors is a standard method of measuring intra-tumoral microvessel density (MVD). Several studies reported that the level of MVD reflects the angiogenesis process in tumor tissues.[27–29] Immunoreactive blood vessels and cells were counted (in a similar way as in oncology studies) in five representative fields, with the use of an eyepiece with a calibrated grid in combination with the 40x objectives. These representative fields were selected based on the presence of immunoreactive blood vessels and cells. With this magnification and calibration, immunoreactive blood vessels and cells present in an area of 0.33 mm $\times$ 0.22 mm were counted.

Rat Streptozotocin-Induced Diabetes Model

All procedures with animals were performed in accordance with the Association for Research in Vision and Ophthalmology (ARVO) statement for use of animals in ophthalmic and vision research and were approved by the institutional Animal Care and Use Commitµtee of the College of Pharmacy, King Saud University. Adult male Sprague Dawley rats of 8-9 weeks of age (200–220 g) were overnight fasted and a single bolus dose of streptozotocin 65 mg/kg in 10 mM sodium citrate buffer, pH 4.5 (Sigma, St. Louis, MO) was injected intraperitoneally. Equal volumes of citrate buffer were injected in age-matched control rats. Rats were considered diabetic if their blood glucose levels were in excess of 250 mg/dl. After 4 or 12 weeks of diabetes, the rats were euthanized by an overdose of chloral hydrate, the eyes were removed, and retinas were isolated and frozen immediately in liquid nitrogen and stored at −80°C until analyzed. Similarly, retinas were obtained from age-matched nondiabetic control rats.

Intravitreal Injection of sCD146 in Normal Rats

Sprague Dawley rats (220–250 g) were kept under deep anesthesia, and sterilized solution of recombinant sCD146 (5 ng/5 µl; Cat No 9709-MA-050, R&D Systems) was injected into the vitreous of the right eye. The left eyes were used as controls and were injected with 5 µl of sterile phosphate-buffered saline (PBS). The animals were sacrificed 4 days after intravitreal injections, and the retinas were carefully dissected, snap frozen in liquid nitrogen, and stored at −80°C until further analyses.

Measurement of Blood–Retinal Barrier Breakdown in Rats

Retinas were analyzed for blood–retinal barrier (BRB) breakdown 4 days after intravitreal injection of sCD146. The BRB breakdown was assessed by intravenous injection of fluorescein isothiocyanate (FITC)-conjugated dextran and tracking of the dye in the retinas, as previously described.[1] Briefly, rats were deeply anesthetized, and then FITC-conjugated dextran (3–5 kDa, Sigma-Aldrich Corp., St. Louis, MO, USA) was injected intravenously (50 mg/kg body weight). After 30 minutes, a blood sample was collected, and each rat was then perfused with PBS. The retinas were carefully removed, weighed, and homogenized to extract the FITC-conjugated dextran. Fluorescence was measured using a spectraMax Gemini-XPSmicroplate reader (Molecular Devices, Sunnyvale, CA, USA) with excitation and emission wavelengths of 485 nm and 538 nm, respectively, with PBS as a blank. Corrections were made by subtracting the autofluorescence of retinal tissue from rats without FITC-conjugated dextran injection. The amount of FITC-conjugated dextran in each retina was calculated from a standard curve of FITC-conjugated dextran in water. For normalization, the retinal FITC-conjugated dextran amount was divided by the retinal weight and by the concentration of FITC-conjugated dextran in the plasma. BRB breakdown was calculated using the following equation, with the results being expressed in µl/g/h.

$$\frac{\text{Retinal FITC} - \text{dextran}\,(\mu\text{g})/\text{retinal weight(g)}}{\text{Plasma FITC} - \text{dextran concentration}\,(\mu\text{g}/\mu\text{L})} * \text{circulation time (h)}.$$

Detection of CD146 in the Retina of Rats by Immunofluorescence Microscopy

Eyes from normal and diabetic rats were embedded in optimal cutting temperature compound and were snap frozen in liquid nitrogen. The frozen tissue blocks were stored at −80°C until analyzed. Eye cryosections (5 µm thick) were fixed in pre-cooled acetone and incubated with 0.3% H_2O_2 solution to block endogenous peroxidase activity. For immunodetection, overnight incubation with rabbit polyclonal anti-CD146 antibody (1:250, ab-228540, Abcam) was performed. After washing, the slides were incubated with

Alexa Fluor 488 labelled goat anti-rabbit IgG at room temperature for 60 min. Sections were counterstained with 4′,6-diamidino-2-phenylindole (DAPI) (Invitrogen, Eugene, Oregon, USA) for visualization of cell nuclei. Immunofluorescence microscopy was performed using an Olympus fully motorized fluorescence microscope (BX61, Olympus Corporation, Tokyo, Japan) at 40X magnification.

Human Retinal Müller Glial Cell and Retinal Microvascular Endothelial Cell Cultures

Human retinal Müller glial cells (MIO-M1) were cultured in Dulbecco's Minimal Essential Medium (DMEM) containing 1 g/L glucose with 10% (v/v) fetal bovine serum and 1% penicillin/streptomycin. Confluent cells were starved overnight in serum-free DMEM to minimize the effects of serum. Subsequently, the cell cultures were either left untreated or stimulated for 24 h. The following stimuli were used: recombinant human sCD146 (50 or 100 ng/ml) (Cat No 9709-MA-050, R&D Systems, Minneapolis, MN, USA) or 300 µM of the hypoxia mimetic agent cobalt chloride ($CoCl_2$) (AVONCHEM Limited, Nacclesfield, Cheshire, UK).

Human retinal microvascular endothelial cells (HRMECs) were purchased from Cell Systems Corporation (Kirkland, WA, USA) and maintained in complete serum-free media (Cat No SF-4Z0–500, Cell System Corporation) supplemented with "Rocket Fuel" (Cat No SF-4Z0–500, Cell System Corporation), "Culture Boost" (Cat No 4CB-500, Cell System Corporation), and antibiotics (Cat No 4Z0–643, Cell System Corporation) at 37°C in a humidified atmosphere with 5% CO_2. We used HRMECs up to passage 8 for all our experiments. Cells at about 80% confluency were starved in a minimal medium (medium supplemented with 0.25% "Rocket Fuel" and antibiotics) overnight to eliminate any residual effects of growth factors. The following stimuli were used: 50 ng/ml recombinant human VEGF (Cat No 293-VE-050, R&D Systems), 300 µM $CoCl_2$ or 50 ng/ml recombinant human tumor necrosis factor- α (TNF-α) (Cat No 210-TA, R&D Systems) in the absence or presence of the MMP inhibitor ONO-4817 (Cat No sc-203139, Santa Cruz Biotechnology, Inc, Santa Cruz, CA, USA) or the nuclear factor-kappa B (NF-κB) inhibitor BAY11-7085 (Cat No sc-202490, Santa Cruz Biotechnology Inc.). After 24 h, cell supernatants were collected and processed for ELISA analysis. Harvested cells were lysed in radioimmunoprecipitation assay (RIPA) lysis buffer (sc-24948, Santa Cruz Biotechnology, Inc.) for Western blot analysis.

Western Blot Analysis of Human Vitreous Fluid, Müller Cell and Human Retinal Microvascular Endothelial Cell Lysates, and Rat Retinas

Retina and cell lysates were homogenized in Western blot lysis buffer [30 mM Tris-HCl; pH 7.5, 5 mM EDTA, 1% Triton X-100, 250 mM sucrose, 1 mM Sodium vanadate, and a complete protease inhibitor cocktail from Roche (Mannheim, Germany)]. After centrifugation of the homogenates (14,000 × g for 15 min, 4°C), protein concentrations were measured in the supernatants (DC protein assay kit; Bio-Rad Laboratories, Hercules, CA). Equal amounts (30-50 µg) of the protein extracts from lysates were subjected to SDS–PAGE and transferred onto nitrocellulose membranes. To determine the presence of sCD146 in the vitreous samples, equal volumes (15 µl) of vitreous samples were boiled in Laemmli's sample buffer (1:1, v/v) under reducing conditions for 10 min and analyzed as described (1–6).

Immunodetection was performed with the use of rabbit polyclonal anti-CD146 antibody (1:1000, ab-228540, Abcam), rabbit monoclonal anti-phospho-extracellular signal-regulated kinase (ERK)1/2 antibody (1:1500, MAB1018, R&D Systems), mouse monoclonal anti-p65 subunit of nuclear factor-kappa B (NF-κB) antibody (1:500, sc-136548, Santa Cruz Biotechnology Inc.), mouse monoclonal anti-intercellular adhesion molecule-1 (ICAM-1) antibody (1:500, sc-8439, Santa Cruz Biotechnology Inc.), mouse monoclonal anti-VEGF antibody (1:750, MAB293, R&D Systems), and rabbit polyclonal anti-phospho-VEGFR-2 (1:11000, ab5472, Abcam). Nonspecific binding sites on the nitrocellulose membranes were blocked (1.5 h, room temperature) with 5% non-fat milk made in Tris-buffered saline containing 0.1% Tween-20 (TBS-T). Three TBS-T washings (5 min each) were performed before the secondary antibody treatment at room temperature for 1 h. To verify equal loading, membranes were stripped and reprobed with β-actin-specific antibody (1:2000, sc-47778, Santa Cruz Biotechnology Inc.). Bands were visualized with the use of high-performance chemiluminescence (G: Box Chemi-XX8 from Syngene, Synoptic Ltd., Cambridge, UK) and the band intensities were quantified with the use of GeneTools software (Syngene by Synoptic Ltd.).

In Vitro Migration Assay

HRMECs were seeded at 1×10^5 cells/well on six-well culture plates and allowed to grow as described above till 80–90% confluency. Quiescence was induced by incubating the cells in minimal media overnight. Using sterile pipette tips, scratches were made, and then cells were rinsed with PBS. Cells were either left untreated or treated either with 100 ng/ml of recombinant sCD146 or 50 ng/ml of recombinant VEGF for 18 h. Cell migration/growth was monitored using an inverted microscope (Olympus IX81, Olympus Corporation, Tokyo, Japan). Analysis of migration/growth was done using Image J software.

Statistical Analysis

Management of the obtained data was preliminarily done using Excel 2013 (Microsoft, Redmond, WA, USA), and then all statistical analyses were performed with the use of the SPSS version 21.0 software (IBM, Armonk, NY, USA). Shapiro-Wilk (S-W) test and normal Q-Q plots were used to test for the normality distribution of the data. When the data were normally distributed, the data were presented as mean ±standard deviation (range). One-way ANOVA and independent t-test were used to compare the groups; and henceforth Pearson correlation coefficients were calculated. When the data were not normally distributed, non-parametric tests (Kruskal-Wallis test, Mann-Whitney test and Spearman's correlation coefficients) were performed and the data were presented as median (interquartile range; IQR; Q1-Q3). A p value less than 0.05 indicated statistical significance.

Investigative Ophthalmology & Visual Science

Results

ELISA Levels of sCD146 and VEGF in Vitreous Samples from Patients with PDR and Nondiabetic Control Patients

We used ELISA to compare sCD146 levels in vitreous samples from 41 patients with PDR with those of 27 nondiabetic controls. sCD146 levels in vitreous samples from PDR patients were significantly higher than the levels in nondiabetic controls ($p < 0.001$; Mann-Whitney test) (Table). Similarly, levels of the angiogenic biomarker VEGF in vitreous samples from PDR patients were significantly higher than the levels in nondiabetic controls ($p = 0.002$; Mann-Whitney test) (Table). Comparisons of sCD146 and VEGF levels among PDR patients with active neovascularization ($n = 12$), PDR patients with involuted neovascularization ($n = 29$), and nondiabetic control patients ($n = 27$) were conducted with the Kruskal-Wallis test. The levels differed significantly between the 3 groups ($p<0.001$ for both comparisons) (Table). Pairwise comparisons (Mann-Whitney test) indicated that sCD146 and VEGF levels were significantly higher in patients with active PDR than in involuted PDR patients ($p = 0.005$; $p = 0.001$, respectively) and control patients ($p<0.001$ for both comparisons). In addition, sCD146 and VEGF levels in patients with inactive PDR were significantly higher than the levels in nondiabetic control patients ($p = 0.006$; $p = 0.018$, respectively). Next, we analyzed the correlation between vitreous fluid levels of sCD146 and the angiogenic factor VEGF. We found a significant positive correlation (Spearman's correlation coefficient) between vitreous fluid levels of sCD146 and levels of VEGF ($r = 0.736$; $p<0.001$) (Fig. 1A).

Western Blot Analysis of Vitreous Samples from Patients with PDR and Nondiabetic Control Patients

With the use of Western blot analysis, we confirmed that sCD146 was present in vitreous samples and sCD146 levels were enhanced in PDR. Densitometric analysis demonstrated a significant increase in sCD146 expression in samples from PDR patients ($n = 10$) compared with samples from control patients ($n = 8$) ($p = 0.005$; Mann-Whitney test) (Figs. 1B, C).

Expression of CD146 in Epiretinal Fibrovascular Membranes From Patients With PDR

To identify the local cellular source of vitreous fluid sCD146 and to examine the tissue localization and expression of CD146, epiretinal fibrovascular membranes from patients with PDR were studied by immunohistochemical analysis. As a negative control, the immunohistochemical staining procedure was performed with omission of the primary antibody from the protocol. No staining was observed in the negative control slides (Fig. 2A). The level of angiogenic activity of epiretinal fibrovascular membranes was determined by staining for the vascular endothelial cell marker CD31. All membranes showed neovessels that were positive for CD31. Representative stainings for CD31 showing new blood vessels in a membrane from a patient with active PDR (Fig. 2B) and in a membrane from a patient with involuted PDR (Fig. 2C) are shown. Leukocytes expressing the leukocyte common antigen CD45 (Fig. 2D) and spindle-shaped myofibroblasts expressing α-SMA (Fig. 2E) were detected in the stromal compartment. Immunoreactivity for CD146 was observed in all membranes. Representative examples of stainings in active (Fig. 3A) and involuted (Fig. 3B) membranes are shown. Immunoreactivity for CD146 was noted in vascular endothelial cells (Figs. 3A, 3B) and stromal cells. Stromal cells were spindle-shaped cells expressing α-SMA (Fig. 3C) and leukocytes co-expressing CD45 (Figs. 3D, 3E).

Correlations Between Expression of CD146 and Angiogenic Activity in Epiretinal Fibrovascular Membranes From Patients With PDR

On the basis of the well-known angiogenic activity of CD146,[18–21] we sought to determine the correlation between the expression of CD146 and angiogenic activity. Significant positive correlations (Pearson's correlation coefficient) were detected between the numbers of blood vessels expressing CD31, reflecting the angiogenic activity of PDR epiretinal fibrovascular membranes, and the numbers of blood vessels ($r = 0.647$; $p = 0.004$) and stromal cells ($r = 0.721$; $p = 0.001$) expressing CD146. The mean numbers of blood vessels expressing CD31 were significantly higher in membranes from patients with active PDR ($n = 11$) (108.0 ± 36.3) than in membranes from patients with involuted PDR ($n = 7$) (35.4 ± 24.6) ($p < 0.001$; independent t-test). Similarly, in membranes from patients with active PDR, the mean numbers of blood vessels (70.0 ± 14.3) and stromal cells (88.6 ± 34.6) expressing CD146 were significantly higher than the numbers of blood vessels (27.6 ± 19.1) and stromal cells (38.3 ± 35.6) expressing CD146 in membranes from patients with involuted PDR ($p < 0.001$; $p = 0.009$, respectively; independent t-test).

Table. Comparisons of VEGF and sCD146 ELISA Levels in Vitreous Samples from Patients with PDR With or Without Active Neovascularization and Nondiabetic Patients With Rhegmatogenous RD

Disease Group	VEGF (pg/mL)	sCD146 (pg/mL)
RD ($n = 27$), median (IQR)	132.4 (54.5–200.0)	79.2 (38.7–119.7)
All PDR ($n = 41$), median (IQR)	567.1 (212.4–1235.1)	234.2 (91.6–322.1)
P (Mann–Whitney test)	0.002*	<0.001*
Active PDR ($n = 12$), median (IQR)	1646.7 (618.6–2147.1)	387.2 (331.3–496.1)
Inactive PDR ($n = 29$), median (IQR)	418.4 (143.7–1075.1)	167.2 (67.6–270.2)
RD ($n = 27$), median (IQR)	132.4 (54.5–200.0)	79.2 (38.7–119.7)
P (Kruskal–Wallis test)	<0.001*	<0.001*

* Statistically significant at 5% level of significance.

Investigative Ophthalmology & Visual Science

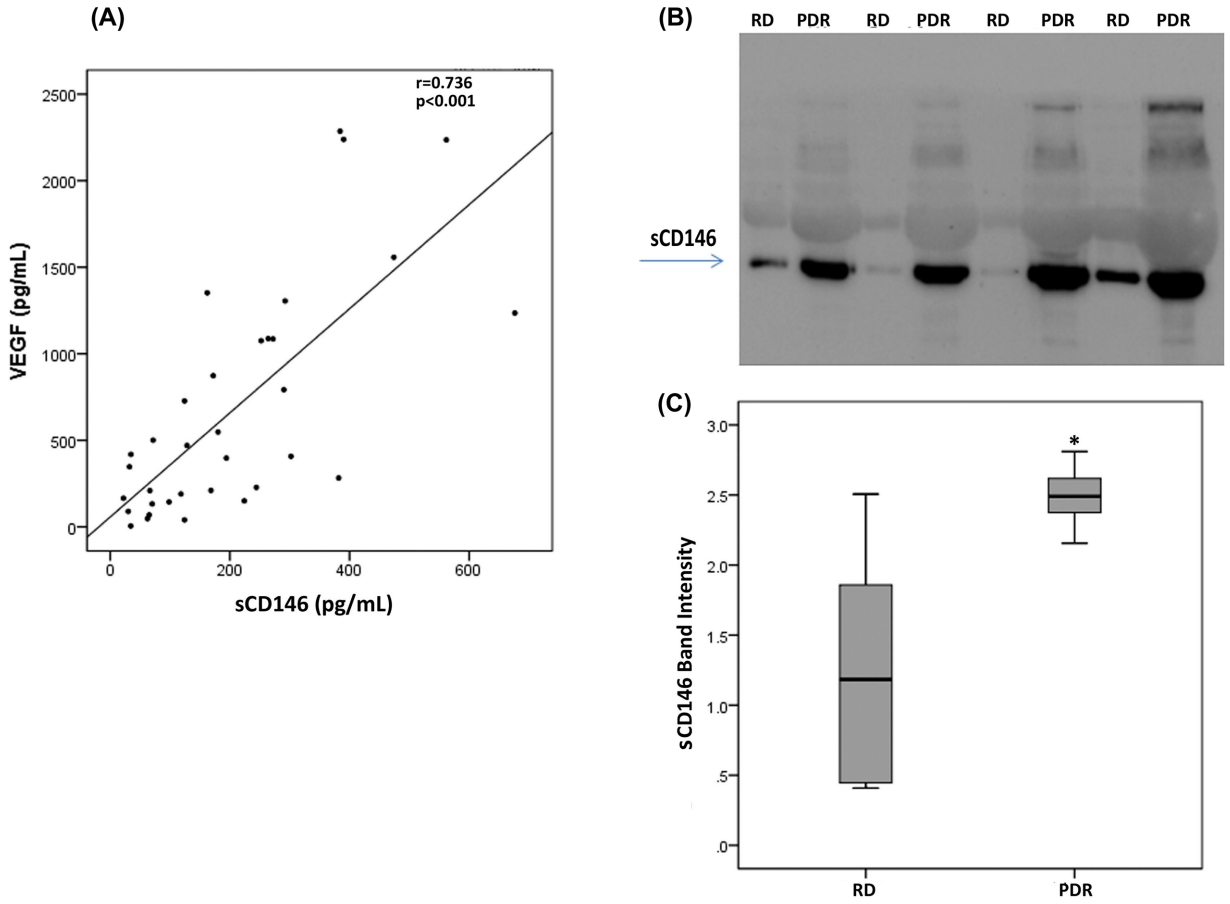

Figure 1. Significant positive correlation between vitreous fluid levels of sCD146 and levels of VEGF (Spearman's correlation coefficient), as measured by specific ELISAs (panel **A**). Determination of sCD146 levels in vitreous fluid samples. Equal volumes (15 µl) of vitreous fluid samples from patients with proliferative diabetic retinopathy (PDR; n = 10) and from nondiabetic patients with rhegmatogenous retinal detachment (RD; n = 8) were subjected to gel electrophoresis and the presence of sCD146 was detected by Western blot analysis. A representative set of samples is shown (panel **B**). The intensity of the protein band was determined in all samples (panel **C**). sCD146 band intensities were compared between the RD and PDR groups. Results are expressed as median (interquartile range). (p = 0.005; Mann-Whitney test).

Expression of CD146 in Epiretinal Fibrocellular Membranes From Patients With PVR

For comparison, we used epiretinal fibrocellular membranes from patients with retinal detachment complicated by PVR. No staining was observed in the negative control slides (Fig. 4A). All membranes showed α-SMA-expressing spindle-shaped myofibroblasts (Fig. 4B) and leukocytes expressing CD45 (Fig. 4C). Immunostaining for CD146 was detected in spindle-shaped α-SMA-expressing myofibroblasts (Fig. 4D). Double immunohistochemistry analysis showed the presence of cells co-expressing CD146 and CD45 (Figs. 4E, 4F). From this analysis we concluded that CD146 expression occured intra-ocularly in various cell types in both PDR and PVR. Together, our data incited the question whether CD146 expression is constitutive or induced by the diabetic process. To assess this *in vivo,* we studied CD146 expression in a rat model of diabetes.

Effect of Diabetes on Retinal Expression of CD146 in Experimental Rats

We analyzed the induction of CD146 in the retina of rats with streptozotocin-induced diabetes. Consistently with our current results in clinical samples, CD146 protein levels increased in the retina of rats after 12 weeks of streptozotocin-induced diabetes. Western blot analysis of homogenized retinal tissue demonstrated a small but significant increase in CD146 in diabetic retinas after 12 weeks of diabetes (n = 12) compared to nondiabetic controls (n = 30). However, the expression of CD146 did not differ significantly between nondiabetic controls and diabetic rat retinas after 4 weeks of diabetes (n = 18). In addition, the expression of CD146 in the retinas from 12 week diabetic rats was significantly higher than the expression in 4 week diabetic rats in line with the progressive character of diabetes development (Fig. 5A). By immunofluorescence microscopy analysis, we demonstrated that retinas of nondiabetic and diabetic rats expressed CD146 in endothelial cells of capillaries, which was consistent with previous reports (Fig. 5B).[14,16] So far, we documented the expression of CD146 in ocular tissues of patients with PDR and PVR and an increase of CD146 retinal expression levels with progression of diabetes in a rat animal model of diabetes. Aside the adhesive functions of intact CD146, this molecule may be shed by proteolysis unleashing cytokine-like functions by the soluble form (sCD146). Above, we documented increased levels of sCD146 in PDR vitreous fluid samples. A logical next step was to study the effects of sCD146 on critical cell types: retinal Müller glial cells and HRMECs.

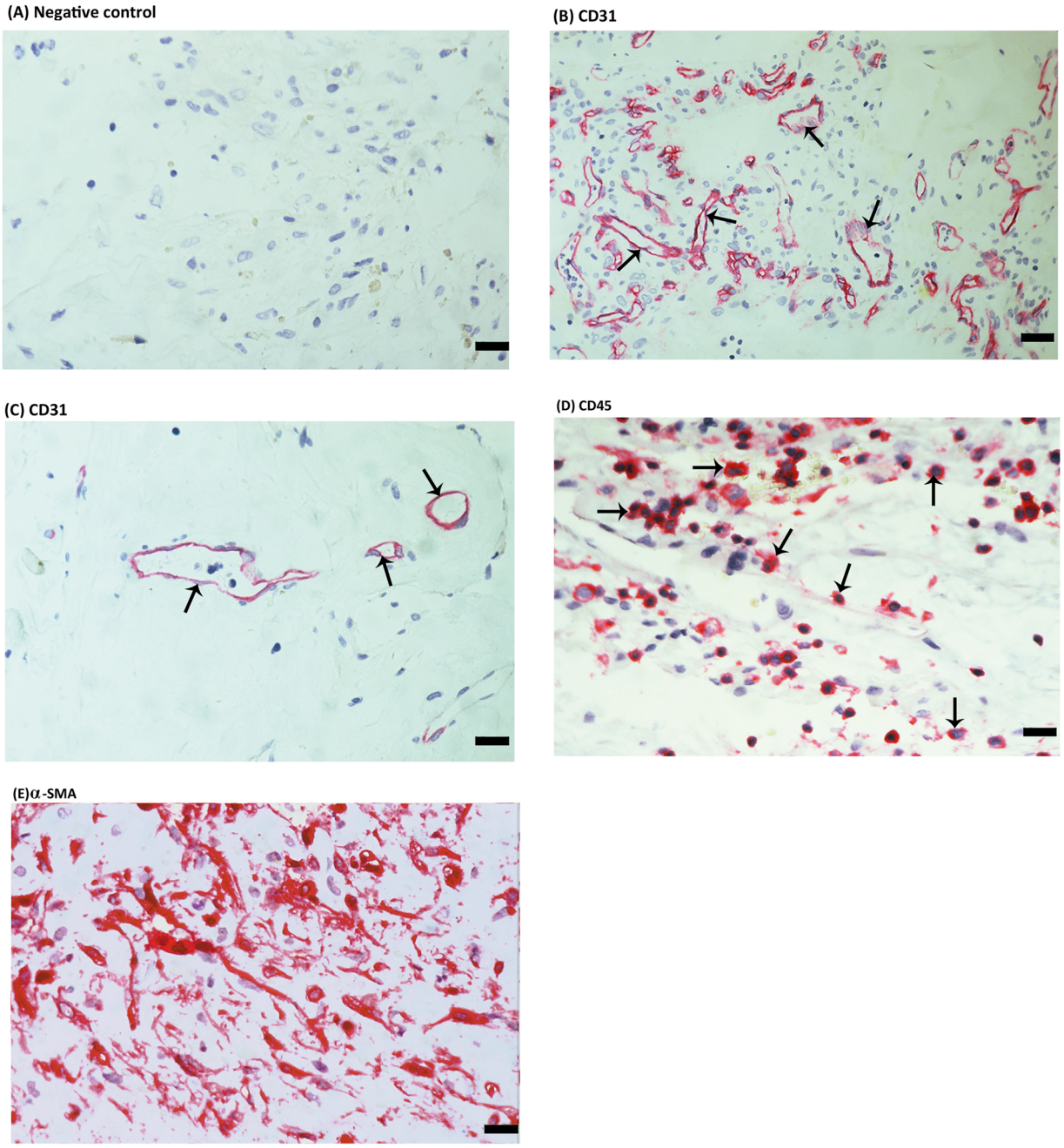

Figure 2. Immunohistochemical staining of proliferative diabetic retinopathy (PDR) epiretinal fibrovascular membranes. (**A**) Negative control slide (procedure without the addition of the primary antibody) showing no labelling. Immunohistochemical staining for the endothelial cell marker CD31 showing pathologic new blood vessels expressing this endothelial cell marker in a membrane from a patient with active neovascularization (arrows) (**B**) and in a membrane from a patient with involuted PDR which is composed mostly of fibrous tissue (arrows) (**C**). Immunohistochemical staining for the leukocyte common antigen CD45 showing infiltrating leukocytes in the stroma (arrows) (**D**). Immunohistochemical staining for α-smooth muscle actin (α-SMA) showing immunoreactivity in spindle-shaped myofibroblasts (**E**) (scale bar, 10 µm).

sCD146 Induces Upregulation of the Proangiogenic Factors VEGF and MMP-9 in Human Retinal Müller Glial Cells

Müller cell-derived VEGF plays an essential role in the development of pathological retinal neovascularization.[30] In view of the correlations between sCD146 and VEGF (Fig. 1) we studied whether CD146 induces downstream angiogenic factors by experiments on Müller cells. ELISA analysis revealed that at 50 or 100 ng/ml, sCD146 significantly increased the levels of VEGF (Fig. 6A) and MMP-9 (Fig. 6B) in the culture media. These data hinted to signaling events activated by sCD146.

sCD146 Induces Upregulation of Phospho-ERK1/2 and the p65 Subunit of NF-κB in Human Retinal Müller Glial Cells

Western blot analysis demonstrated that treatment of Müller cells with sCD146 (100 ng/ml) induced significant upregulation of the protein levels of the p65 subunit of NF-κB

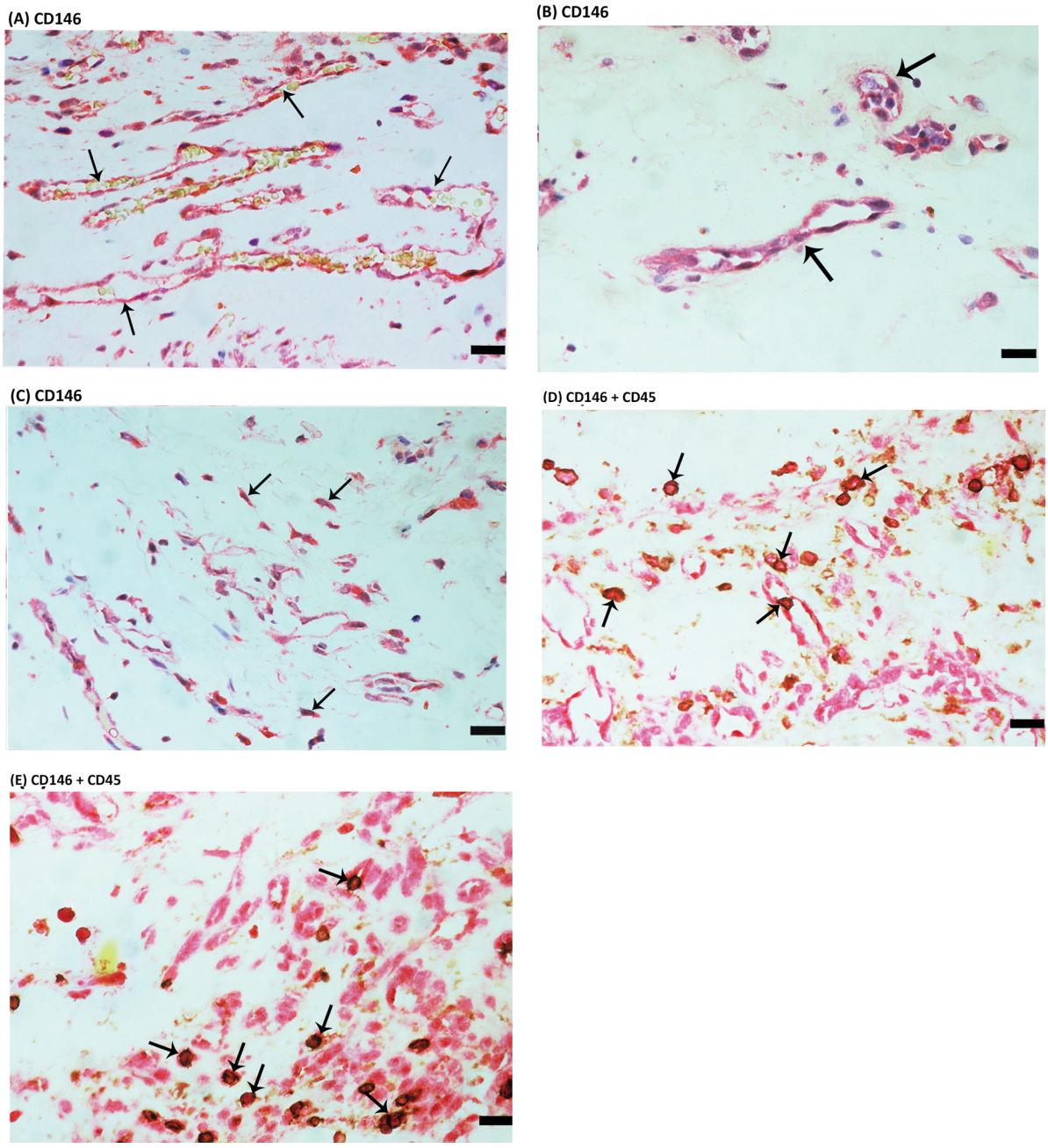

Figure 3. Immunohistochemical staining of proliferative diabetic retinopathy (PDR) epiretinal fibrovascular membranes. Immunohistochemical staining for CD146 showing immunoreactivity in vascular endothelial cells in a membrane from a patient with active PDR (**A**) and in a membrane from a patient with involuted PDR (arrows) (**B**). Immunoreactivity for CD146 was also detected in stromal spindle-shaped myofibroblasts (arrows) (**C**). Double immunohistochemical staining for CD45 (brown) and CD146 (red) demonstrating stromal cells co-expressing CD45 and CD146. No counterstain to visualize the cell nuclei was applied (arrows) (**D**, **E**) (scale bar, 10 µm).

(Fig. 6C) and phospho-ERK1/2 (Fig. 6D). However, 50 ng/ml sCD146 treatment did not affect the expression of phospho-ERK1/2 and the p65 subunit of NF-κB (data not shown). Exposure of Müller cells to sCD146 did not affect the expression of phospho-VEGFR-2 (data not shown). With the use of Western blot analysis we determined that Müller cells do not express CD146. Treatment of Müller cells with the hypoxia mimetic agent $CoCl_2$ did not induce the expression of CD146 (data not shown).

Proinflammatory Cytokine TNF-α Induces Upregulation of sCD146 in Human Retinal Microvascular Endothelial Cells

To confirm the observed expression of CD146 by endothelial cells in epiretinal fibrovascular membranes from patients with PDR, we performed *in vitro* experiments on HRMECs. We showed that HRMECs express CD146 but TNF-α did not alter this expression level (Fig. 7A). With the use of

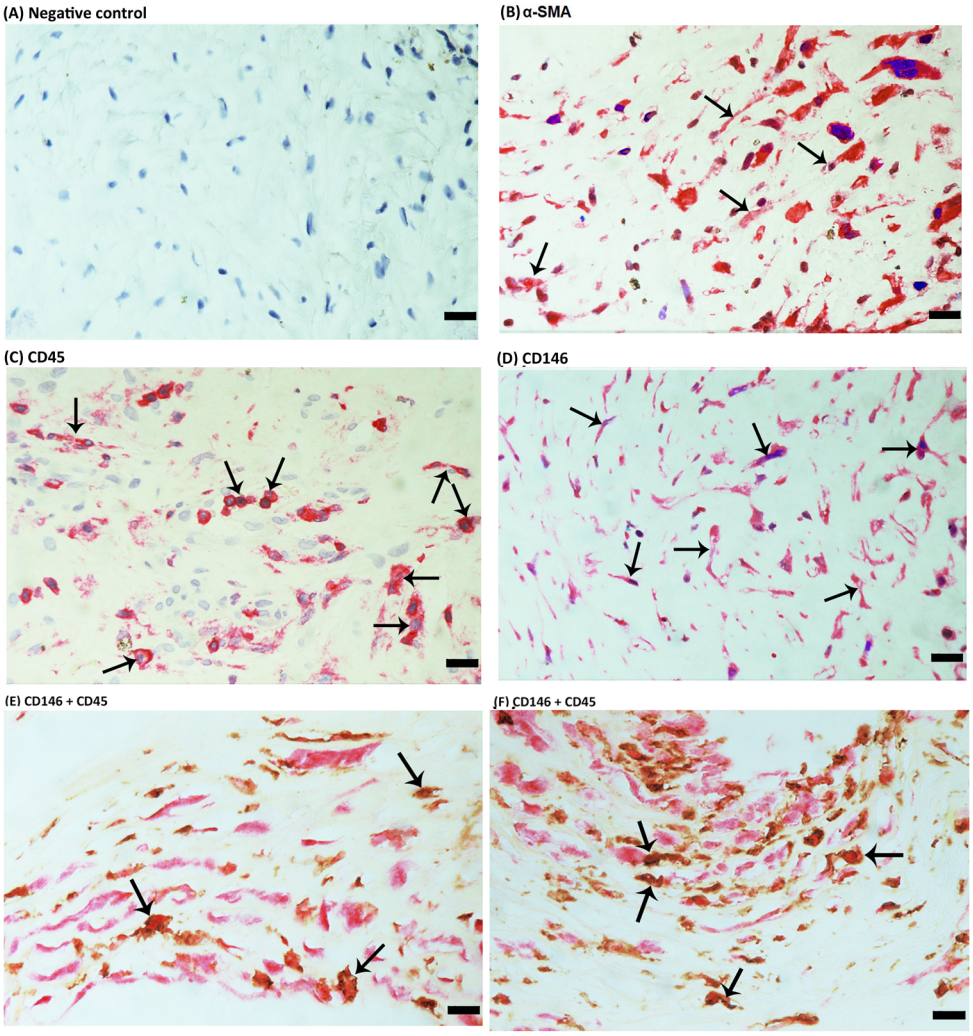

Figure 4. Immunohistochemical staining of proliferative vitreoretinopathy epiretinal fibrocellular membranes. Negative control slide showing no staining (**A**). Immunohistochemical staining for α-smooth muscle actin (α-SMA) showing immunoreactivity in myofibroblasts (arrows) (**B**). Immunohistochemical staining for CD45 showing immunoreactivity in leukocytes (arrows) (**C**). Immunohistochemical staining for CD146 showing immunoreactivity in spindle-shaped myofibroblasts (arrows) (**D**). Double immunohistochemistry for CD45 (brown) and CD146 (red) showing cells co-expressing CD45 and CD146. No counterstain to visualize the cell nuclei was applied (arrows) (**E**, **F**) (scale bar, 10 µm).

Western blot analysis, we demonstrated that treatment with TNF-α (50 ng/ml) significantly increased the levels of shed sCD146 in the culture medium as compared to untreated control (Fig. 7B). Our results suggested that sCD146 in the vitreous fluid may originate from the proteolytical shedding of the membrane-bound CD146 on blood-retinal barrier endothelial cells during inflammation. With the knowledge that CD146 shedding is mediated by metalloprotease activity,[15] we tried to corroborate this mechanism in vitro.

Matrix Metalloproteinase Inhibitor ONO-4817 Attenuates TNF-α-Induced Upregulation of sCD146 in Human Retinal Microvascular Endothelial Cells

To confirm the involvement of MMPs in TNF-α-induced upregulation of sCD146, we treated HRMECs with TNF-α (50 ng/ml) or with TNF-α (50 ng/ml) plus the MMP inhibitor ONO-4817 (10 µM). ELISA analysis revealed that treatment of HRMECs with the proinflammatory cytokine TNF-α (50 ng/ml) significantly increased the levels of sCD146 in the culture medium as compared to untreated control. Co-treatment of HRMECs with TNF-α plus ONO-4817 significantly attenuated TNF-α-induced upregulation of sCD146, indicating that TNF-α-promoted CD146 shedding is dependent on MMPs (Fig. 7C). In addition, the NF-κB inhibitor BAY11-7085 (1 or 10 µM) did not affect TNF-α-induced upregulation of sCD146 (data not shown).

Hypoxia Mimetic Agent $CoCl_2$ and the Proangiogenic Factor VEGF Induce Upregulation of sCD146 in Human Retinal Microvascular Endothelial Cells

To investigate the potential role of hypoxia and the proangiogenic factor VEGF in induction of sCD146 and to confirm the significant positive correlation between vitreous fluid levels of VEGF and the levels of sCD146,

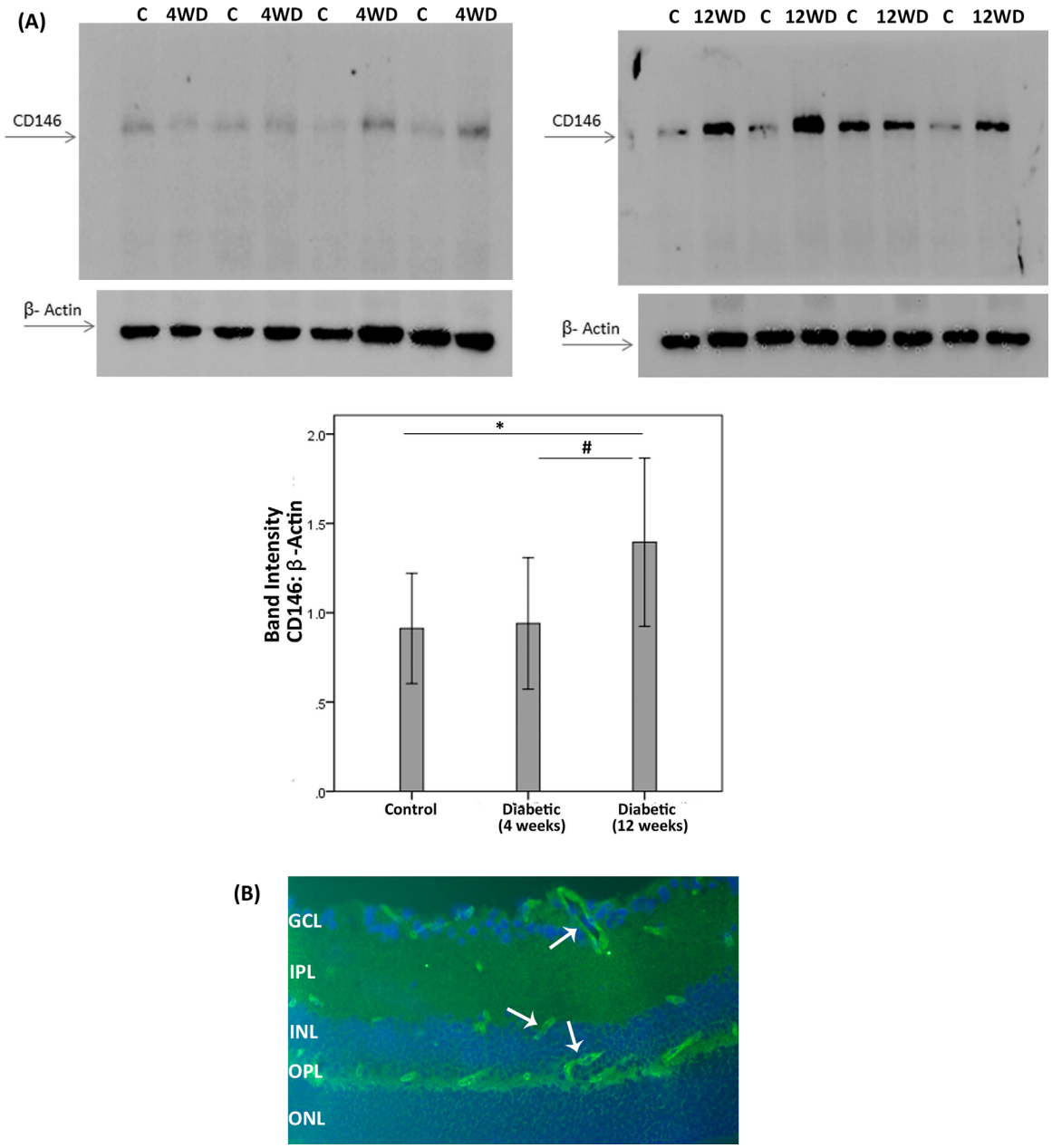

Figure 5. CD146 protein expression in the retinas of diabetic rats. (**A**) CD146 protein expression was determined by Western blot analysis on lysates of diabetic (D) and nondiabetic control retinas (C) at 4 weeks (4W) and 12 weeks (12W) after diabetes induction. After determination of the intensity of the CD146 protein band, intensities were adjusted to those of β-actin in the sample. Results are expressed as mean ±SD. One-way ANOVA and independent t-tests were used for comparisons between the three and two groups, respectively. *$p < 0.05$ compared with the values obtained from nondiabetic controls. #$p < 0.05$ compared with 4 week diabetic rats. (**B**) Immunofluorescence detection of CD146 (light green) in 8-week diabetic rat retina. CD146 immunoreactivity is detected in endothelial cells of the capillaries (white arrows). Nuclei were counterstained with DAPI (blue). GCL = ganglion cell layer; IPL = inner plexiform layer; INL = inner nuclear layer; OPL = outer plexiform layer; ONL = outer nuclear layer.

we performed induction experiments on HRMECs with the hypoxia mimetic agent $CoCl_2$ or VEGF. ELISA analysis revealed that treatment of HRMECs with $CoCl_2$ (300 µM) (Fig. 7D) or VEGF (50 ng/ml) (Fig. 7E) significantly increased the levels of sCD146 in the culture medium as compared to untreated control. However, Western blot analysis of cell lysates demonstrated that VEGF did not affect the expression of the membrane form (data now shown).

sCD146 Induces Migration of Human Retinal Microvascular Endothelial Cells

The migration of endothelial cells plays an important event in the process of angiogenesis. The proangiogenic potential of sCD146 was evaluated with the *in vitro* migration assay. We showed that 100 ng/ml of sCD146 significantly increased the migration of HRMECs (Fig. 8). An optimal dose of VEGF was used as a positive control.

Investigative Ophthalmology & Visual Science

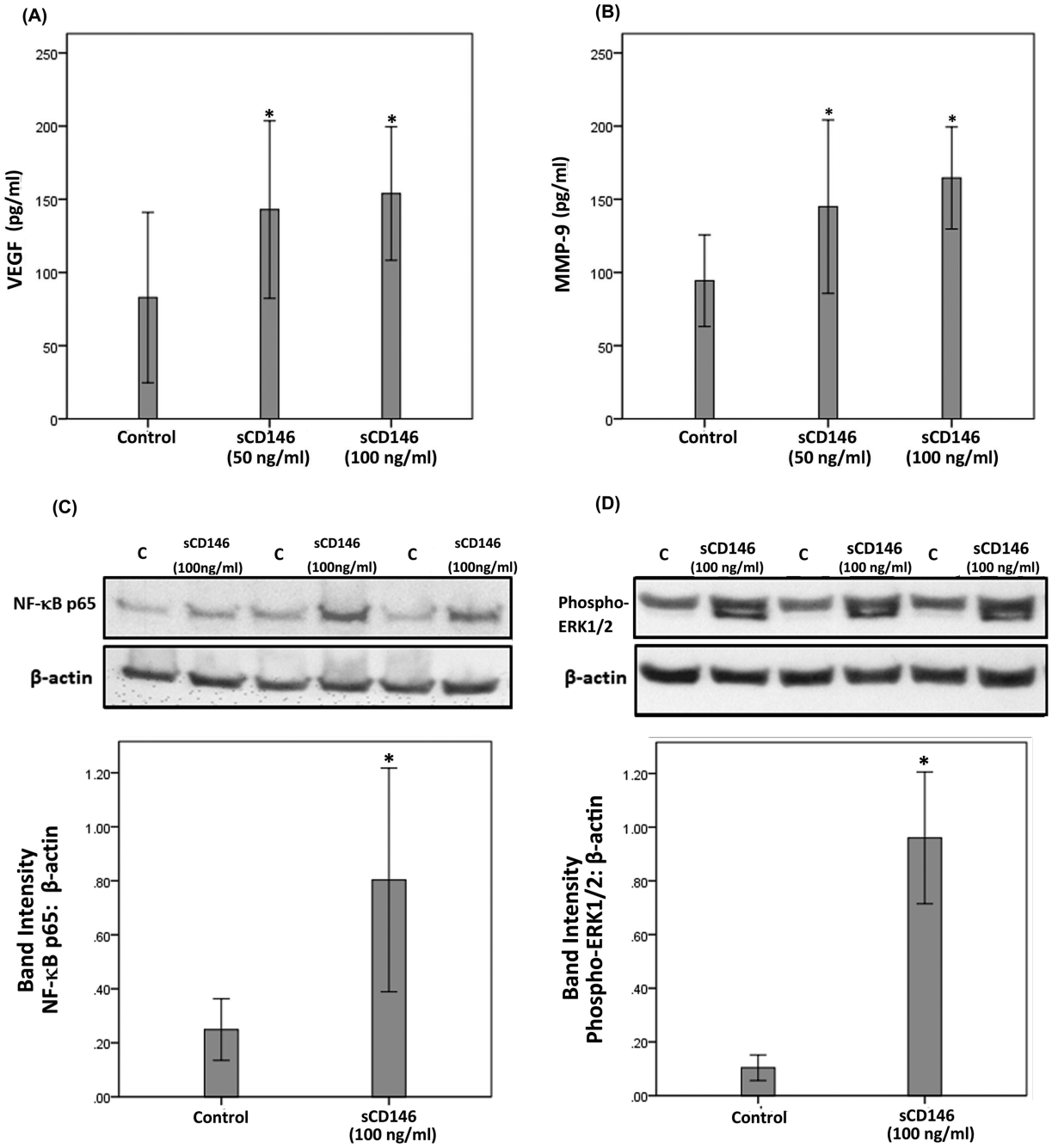

Figure 6. Müller cells were left untreated or treated with sCD146 (50 ng/ml) or sCD146 (100 ng/ml) for 24 hours. Levels of VEGF (panel **A**) and MMP-9 (panel **B**) were quantified in the culture media by ELISA. Results are expressed as mean ±SD from three different experiments. One-way ANOVA and independent t-tests were used for comparisons between the three groups and two groups, respectively. *$p < 0.05$ compared with values obtained from untreated cells. Müller cells were left untreated or treated with sCD146 (100 ng/ml) for 24 hours. Protein expression of the p65 subunit of NF-κB (panel **C**) and phospho-ERK1/2 (panel **D**) in the cell lysates was determined by Western blot analysis. Results are expressed as mean ±SD from three different experiments. (*$p < 0.05$ independent t-test).

Effect of Intravitreal Administration of sCD146 on Blood–Retinal Barrier and on Retinal Expression of Phospho-ERK1/2, the p65 Subunit of NF-κB, ICAM-1 and VEGF in Normal Rats

Fluorescein isothiocyanate-conjugated dextran was used to investigate the extent of retinal vascular permeability. Fig. 9A shows that intravitreal injection of sCD146 significantly increased retinal vascular permeability compared with observations in vehicle (PBS)-injected eyes. Western blot analysis of homogenized retinal tissue revealed that intravitreal injection of sCD146 induced significant upregulation of the protein levels of phospho-ERK1/2 (Fig. 9B), ICAM-1 (Fig. 9C) and VEGF (Fig. 9D) compared to the values obtained from the contralateral eye that received PBS alone. However, sCD146 did not affect the expression of the p65 subunit of NF-κB (data not shown).

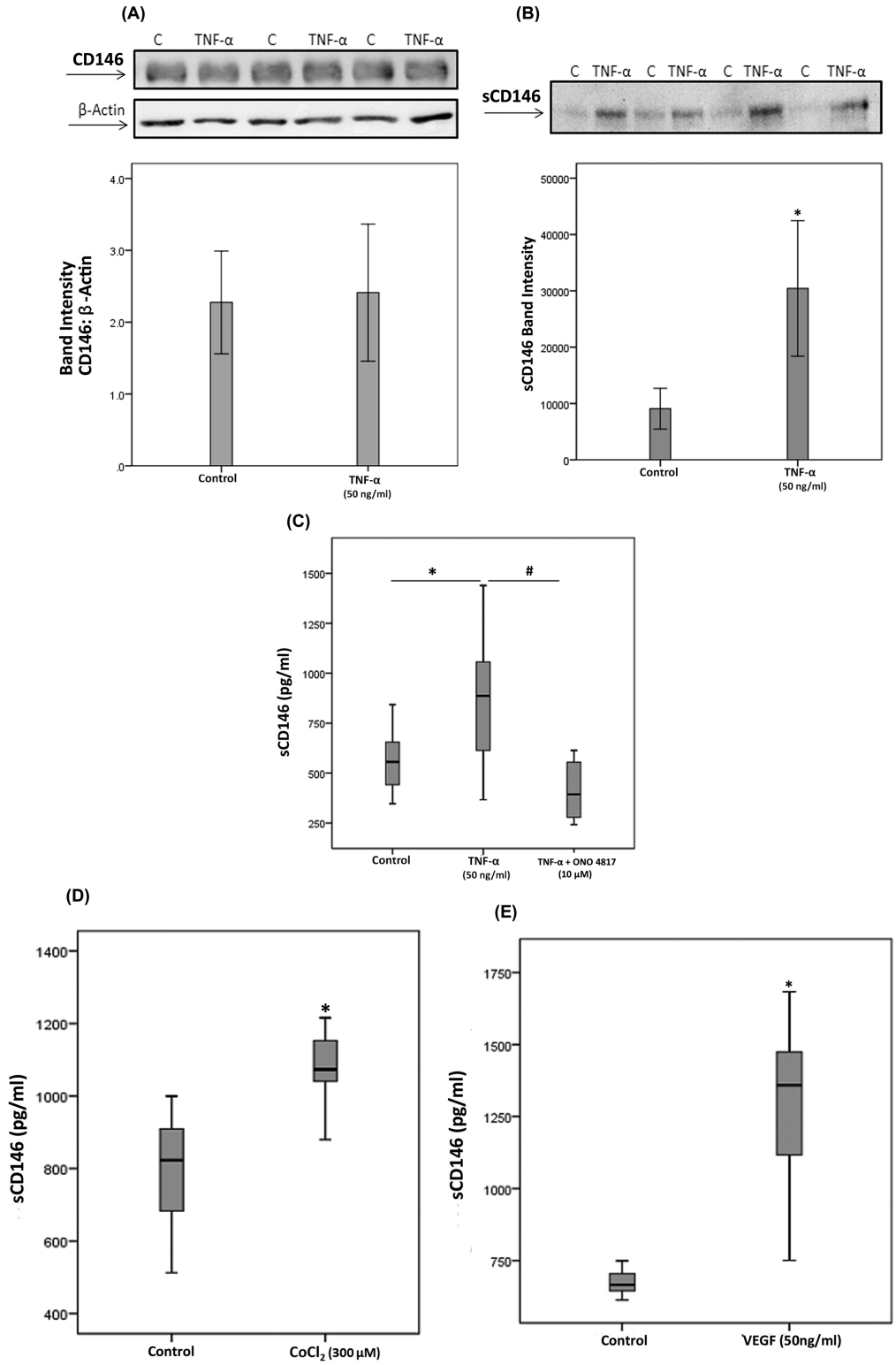

Figure 7. Human retinal microvascular endothelial cells (HRMECs) were left untreated or treated with tumor necrosis factor-α (TNF-α) (50 ng/ml) for 24 hours. Protein expression of CD146 in cell lysate was determined by Western blotting (panel **A**). Levels of sCD146 were quantified in the culture media by Western blot analysis (panel **B**). Results are expressed as mean ±SD from three different experiments (*$p < 0.05$; independent t-test). HRMECs were left untreated or treated with tumor necrosis factor-α (TNF-α) (50 ng/ml) or TNF-α (50 ng/ml) plus ONO-4817 (10 μM) (panel **C**). Levels of sCD146 were quantified in the culture media by ELISA. Results are expressed as median (interquartile range) from three different experiments. Kruskal-Wallis test and Mann-Whitney tests were used for comparisons between three groups and two groups, respectively. *$p < 0.05$ compared with values obtained from untreated cells. #$p < 0.05$ compared

with TNF-α-plus ONO-4817-treated cells. HRMECs were left untreated or treated with cobalt chloride ($CoCl_2$) (300 μM) (panel **D**) or vascular endothelial growth factor (VEGF) (50 ng/ml) (panel **E**) for 24 hours. Levels of sCD146 were quantified in the culture media by ELISA. Results are expressed as median (interquartile range) from three different experiments (*p < 0.05; Mann-Whitney test).

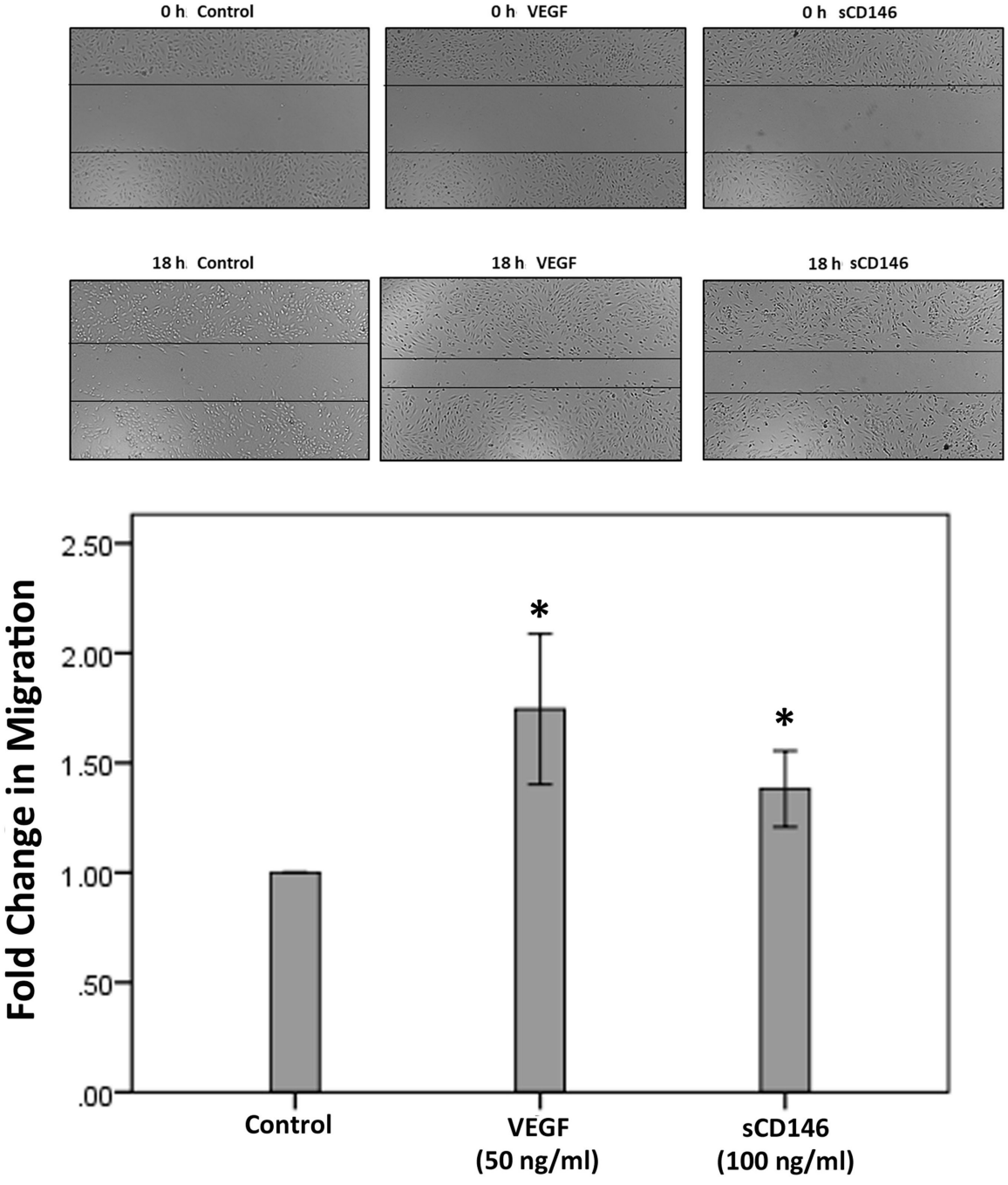

Figure 8. Effects of sCD146 and vascular endothelial growth factor (VEGF) on the migration of human retinal microvascular endothelial cells (HRMECs). Overnight starved HRMECs were left untreated or treated either with sCD146 (100 ng/ml) or with VEGF (50 ng/ml) for 18 h. Cells were visualized using an inverted microscope. Two independent experiments were performed. Each experiment was done in duplicate and 6-8 independent field images were taken for the migration analysis which was done by using Image J software. In the figure, one representative image is illustrated, and the bar graphs show the analysis of all the images from each group represented as fold change in migration versus control. Results are expressed as mean ±SD (*p < 0.05; independent t-test).

Investigative Ophthalmology & Visual Science

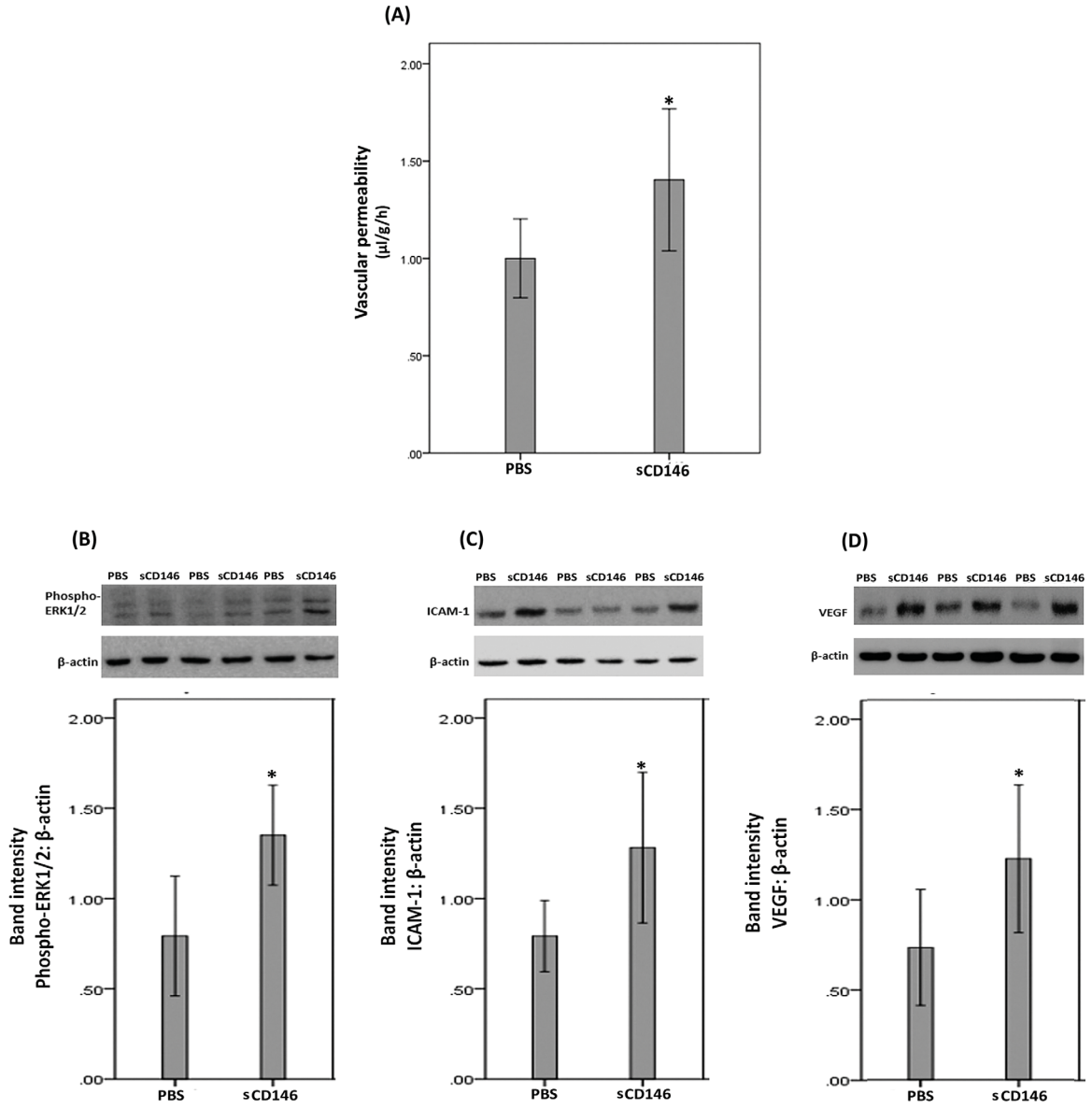

Figure 9. sCD146 induces blood-retinal barrier (BRB) breakdown (panel **A**). sCD146 was injected intravitreally at the dose of 5 ng/5 µl in one eye and the same volume of phosphate-buffered saline (PBS) was injected in the contralateral eye of normal rats. The BRB was quantified with the fluorescein isothiocyanate-conjugated dextran technique. Results are expressed as mean ± SD of 13 rats. *$p < 0.05$ compared to the values obtained from PBS-injected eyes (independent t-test). Western blot analysis of rat retinas revealed that intravitreal administration of sCD146 (5 ng/5 µL) induced significant upregulation of the expression of phospho-ERK1/2 (panel **B**), intercellular adhesion molecule-1 (ICAM-1) (panel **C**) and vascular endothelial growth factor (VEGF) (panel **D**) compared to intravitreal administration of PBS. Results are expressed as mean ±SD from three different experiments (*$p < 0.05$; independent t-test).

Discussion

In the present study, we showed cell biological, biochemical, preclinical and clinical data about the membrane-bound and soluble forms of CD146 in relation to diabetic retinopathy. sCD146 levels were significantly upregulated in vitreous fluid samples and CD146 was expressed in epiretinal fibrovascular membranes from patients with PDR. In addition, CD146 was significantly upregulated in the retina of diabetic rats. Similarly, CD146 expression levels are elevated in the retinas of a murine model of oxygen-induced retinopathy.[18] Using immunohistochemical analysis, we showed that CD146 protein was specifically localized in endothelial cells of pathologic new blood vessels, leukocytes expressing the leukocyte common antigen CD45 and myofibroblasts in epiretinal fibrovascular membranes from patients with PDR. To corroborate the findings at the cellular level, we demonstrated that CD146 was expressed by cultured HRMECs. In the present study, we also demonstrated that the vitreous fluid levels of sCD146 were significantly higher in eyes with active neovascularization in comparison with eyes with involuted disease. In addition, significant positive correlations were observed between the expression levels of CD146 and the levels of angiogenic

Investigative Ophthalmology & Visual Science

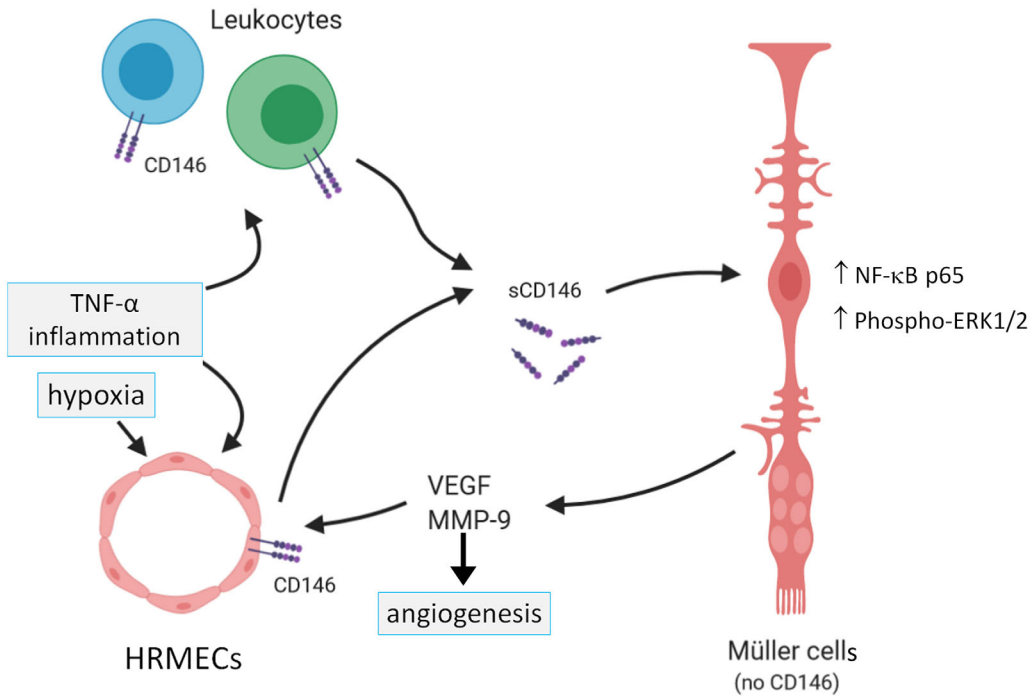

Figure 10. Summary of documented molecular interactions in the regulation of sCD146 production by human retinal microvascular endothelial cells (HRMECs) and its effect on retinal Müller glial cells in switching on angiogenic signals. TNF-α = tumor necrosis factor-alpha; VEGF = vascular endothelial growth factor; MMP-9 = matrix metalloproteinase-9; ERK = extracellular-signal regulated kinase; NF-κB = nuclear factor-kappa B.

activity in PDR epiretinal fibrovascular membranes. Vitreous sCD146 appears to be produced locally as a result of MMP-dependent shedding of membrane-bound CD146[15,24] on endothelial cells, leukocytes and myofibroblasts. In previous studies, we demonstrated increased levels of several MMPs including MMP-1, MMP-7, MMP-9 and MMP-14 in the ocular microenvironment of patients with PDR.[2,5]

Several studies highlighted CD146 as a key actor of tumor growth and angiogenesis.[13,14,16,17,19,21] CD146 interacts directly with VEGFR-2 in endothelial cells and functions as a coreceptor for VEGFR-2 to enhance VEGF-induced angiogenesis[16]. CD146 inhibition decreases VEGF-induced phosphorylation of VEGFR-2 and activation of NF-κB in endothelial cells.[16,17] In addition, inhibiting CD146 significantly impaired VEGF-induced endothelial cell migration and tube formation, *in vivo* angiogenesis and tumor growth.[16,17,19] Inhibition of CD146 also significantly attenuates retinal neovascularization in a murine model of oxygen-induced retinopathy.[18] Moreover, combination therapy with anti-CD146 antibody and anti-VEGF antibody showed an additive inhibitory effect in the treatment of several tumors.[16] Furthermore, CD146 deficiency was associated with reduced VEGF-induced vessel permeability *in vivo*.[31] Our present data about VEGF and sCD146 signaling in endothelial cells *in vitro* and *in vivo* provided complementary mechanistic insights about diabetic retinopathy.

In addition to the membrane form of CD146, sCD146 was demonstrated to display angiogenic properties. In vitro, sCD146 enhances angiogenic characteristics of endothelial progenitor cells, leading to increased cell migration, proliferation and the capacity to establish capillary-like structures. In addition, sCD146 enhances VEGFR-2 expression and VEGF secretion.[20] CD146-positive cancer cells secrete sCD146 that promotes tumor angiogenesis and tumor cell proliferation and survival. Moreover, sCD146 induces increased expression of the pro-angiogenic factors MMP-9 and VEGF in cancer cells.[21] Local injection of sCD146 *in vivo* significantly increases vascularization in a rat model of hind-limb ischemia.[20] In addition, administration of a monoclonal antibody specifically targeting sCD146 decreases growth and vascularization and increases apoptosis of CD146-positive tumors.[21] In agreement with these studies, we demonstrated that sCD146 induced HRMECs migration *in vitro*, a crucial step in the angiogenesis cascade. Our analysis showed a significant positive correlation between the vitreous fluid levels of sCD146 and those of the angiogenic factor VEGF, a key angiogenic factor in PDR.[9] These findings suggest that co-expression of these factors is mechanistically interrelated. To corroborate the findings at the cellular level and in line with the mentioned previous studies, we demonstrated for the first time the capability of sCD146 to target Müller cells and to induce signaling by activation of the extracellular signal regulated kinase ERK1/2 and the proinflammatory transcription factor NF-κB towards the synthesis and secretion of the proangiogenic factors VEGF and MMP-9. Müller cells are known to be the major source of VEGF secretion and therefore contribute to the development of pathological retinal angiogenesis.[30] Additionally, intravitreal administration of sCD146 induced a significant upregulation of phospho-ERK1/2 and VEGF in the retina of normal rats and breakdown of the BRB. Our findings suggested that sCD146-induced BRB breakdown might be related to upregulation of VEGF, a major contributor to BRB breakdown in diabetes.[9] Reciprocally, we

Investigative Ophthalmology & Visual Science

demonstrated that treatment of HRMECs with the hypoxia mimetic agent $CoCl_2$ or VEGF induced significant upregulation of sCD146 in the culture medium.

In the present study, we demonstrated the presence of leukocytes expressing CD146 in PDR and PVR epiretinal membranes. Apart from its role in angiogenesis, several studies suggested that the CD146/sCD146 pathway has proinflammatory properties that promote the development of inflammation and leukocyte transmigration. sCD146 levels are elevated in the synovial fluid of patients with rheumatoid arthritis[32] in the cerebrospinal fluid of patients with neuroinflammatory disease[22,23] and in the serum of patients with systemic sclerosis.[33] Levels of sCD146 in the cerebrospinal fluid significantly correlate with the hyperpermeability-related clinical parameters of blood-brain barrier dysfunction and neuroinflammation-related factors[22,23]. In experimental autoimmune encephalomyelitis, an animal model of multiple sclerosis, endothelial CD146 is actively involved in the transmigration of lymphocytes across the blood-brain barrier and promotes the formation of central nervous system lesions. Selectively deleting CD146 expression in vascular endothelial cells or blocking endothelial CD146 with a specific antibody causes a significant reduction in the infiltration of pathogenic lymphocytes into the central nervous system and decreases neuroinflammation.[25]

The proinflammatory cytokine TNF-α increases CD146 expression on endothelial cells and induces significant elevation of sCD146 in the culture medium of endothelial cells. TNF-α-induced shedding of sCD146 is MMP-dependent.[23,24] Similarly, we observed that treatment of HRMECs with the proinflammatory cytokine TNF-α induced significant upregulation of sCD146 in the culture medium and that addition of the potent broad-spectrum MMP inhibitor ONO-4817 reduced sCD146 release. Mechanistic studies have shown that TNF-α-induced upregulation of CD146 is mediated through NF-κB activation.[18] However, in the present study, the NF-κB inhibitor BAY11-7085 did not attenuate TNF-α-induced upregulation of sCD146 in HRMECs. In *in vitro* models, sCD146 promoted blood-brain barrier permeability[22] and both membrane and soluble forms of CD146 are involved in leukocyte transmigration through the endothelial monolayer.[23,24] In addition, treatment of endothelial cells with sCD146 induced activation of the proinflammatory transcription factor NF-κB and the expression of the adhesion molecules ICAM-1 and vascular cell adhesion molecule-1, both of which play an important role in promoting leukocyte transmigration.[23] Enhanced adhesion of circulating leukocytes to the retinal microvascular endothelium is a crucial element for the development of retinal endothelial cell damage, breakdown of the BRB and capillary nonperfusion.[34] In this study, we demonstrated that intravitreal injection of sCD146 in normal rats induced significant upregulation of ICAM-1 in the retina and breakdown of the BRB.

In conclusion, the proangiogenic and proinflammatory CD146/sCD146 pathway is upregulated and provides multiple molecular and cellular interactions (Fig. 10) in the intraocular microenvironment of patients with PDR, particularly in patients with active angiogenesis. Our findings contribute new insights about the molecular biology of CD146 and suggest that this pathway is involved in the initiation and progression of PDR and could serve as a potential therapeutic target in combination with anti-VEGF agents in PDR patients.

Acknowledgments

The authors thank Connie B. Unisa-Marfil for secretarial assistance; Wilfried Versin, Pierre Fiten, Kathleen Van Den Eynde and Saleh Hashem Aljowied, for technical assistance.

Supported by King Saud University through Vice Deanship of Research Chair (Dr. Nasser Al-Rashid Research Chair in Ophthalmology; AMA) and by Research Foundation of Flanders and KU Leuven C1 funding (2017–2023, project 17/17/010; GO).

Human retinal Müller glial cells (MIO-M1) were a generous gift from Astrid Limb, PhD, Institute of Ophthalmology, University College London, UK.

Disclosure: **A.M. Abu El-Asrar,** None; **M.I. Nawaz,** None; **A. Ahmad,** None; **M.M. Siddiquei,** None; **E. Allegaert,** None; **P.W. Gikandi,** None; **G. De Hertogh,** None; **G. Opdenakker,** None

References

1. Abu El-Asrar AM, Ahmad A, Siddiquei MM, et al. The proinflammatory and proangiogenic macrophage migration inhibitory factor is a potential regulator in proliferative diabetic retinopathy. *Front Immunol*. 2019;10:2752.
2. Abu El-Asrar AM, Mohammad G, Nawaz MI, et al. Relationship between vitreous levels of matrix metalloproteinases and vascular endothelial growth factor in proliferative diabetic retinopathy. *PLoS One*. 2013;8(12):e85857.
3. Abu El-Asrar AM, Alam K, Nawaz MI, et al. Upregulated expression of heparanase in the vitreous of patients with proliferative diabetic retinopathy originates from activated endothelial cells and leukocytes. *Invest Ophthalmol Vis Sci*. 2015;56(13):8239–8247.
4. Abu El-Asrar AM, Ahmad A, Allegaert E, et al. Galectin-1 studies in proliferative diabetic retinopathy. *Acta Ophthalmol*. 2020;98(1):e1–e12, https://doi.org/10.1111/aos.14191.
5. Abu El-Asrar AM, Mohammad G, Allegaert E, et al. Matrix metalloproteinase-14 is a biomarker of angiogenic activity in proliferative diabetic retinopathy. *Mol Vis*. 2018;24:394–406.
6. Abu El-Asrar AM, Struyf S, Mohammad G, et al. Osteoprotegerin Is a New Regulator of Inflammation and Angiogenesis in Proliferative Diabetic Retinopathy. *Invest Ophthalmol Vis Sci*. 2017;58(7):3189–3201, https://doi.org/10.1167/iovs.16-20993.
7. Aguilar-Cazares D, Chavez-Dominguez R, Carlos-Reyes A, Lopez-Camarillo C, Hernadez de la Cruz ON, Lopez-Gonzalez JS. Contribution of Angiogenesis to Inflammation and Cancer. *Front Oncol*. 2019;9:1399, https://doi.org/10.3389/fonc.2019.01399.
8. Neagu M, Constantin C, Caruntu C, Dumitru C, Surcel M, Zurac S. Inflammation: A key process in skin tumorigenesis. *Oncol Lett*. 2019;17(5):4068–4084, https://doi.org/10.3892/ol.2018.9735.
9. Miller JW, Le Couter J, Strauss EC, Ferrara N. Vascular endothelial growth factor A in intraocular vascular disease. *Ophthalmology*. 2013;120(1):106–114, https://doi.org/10.1016/j.ophtha.2012.07.038.
10. Shibuya M. Differential roles of vascular endothelial growth factor receptor-1 and receptor-2 in angiogenesis. *J Biochem Mol Biol*. 2006;39(5):469–478.
11. Salam A, Mathew R, Sivaprasad S. Treatment of proliferative diabetic retinopathy with anti-VEGF agents. *Acta Ophthalmol*. 2011;89(5):405–411.
12. Dorrell MI, Aguilar E, Scheppke L, Barnett FH, Friedlander M. Combination angiostatic therapy completely inhibits ocular and tumor angiogenesis. *Proc Natl Acad Sci USA*. 2007;104(3):967–972.

13. Zeng P, Li H, Lu PH, et al. Prognostic value of CD146 in solid tumor: A Systematic Review and Meta-analysis. *Sci Rep*. 2017;7(1):4223.
14. Stalin J, Nollet M, Dignat-George F, Bardin N, Blot-Chabaud M. Therapeutic and Diagnostic Antibodies to CD146: Thirty Years of Research on Its Potential for Detection and Treatment of Tumors. *Antibodies (Basel)*. 2017;6(4): 17.
15. Bardin N, Francès V, Combes V, Sampol J, Dignat-George F. CD146: biosynthesis and production of a soluble form in human cultured endothelial cells. *FEBS Lett*. 1998;421(1):12–14.
16. Jiang T, Zhuang J, Duan H, et al. CD146 is a coreceptor for VEGFR-2 in tumor angiogenesis. *Blood*. 2012;120(11):2330–2339.
17. Zeng Q, Wu Z, Duan H, et al. Impaired tumor angiogenesis and VEGF-induced pathway in endothelial CD146 knockout mice. *Protein Cell*. 2014;5(6):445–456.
18. Wang P, Luo Y, Duan H, et al. MicroRNA 329 suppresses angiogenesis by targeting CD146. *Mol Cell Biol*. 2013;33(18):3689–3699.
19. Yan X, Lin Y, Yang D, et al. A novel anti-CD146 monoclonal antibody, AA98, inhibits angiogenesis and tumor growth. *Blood*. 2003;102(1):184–191.
20. Harhouri K, Kebir A, Guillet B, et al. Soluble CD146 displays angiogenic properties and promotes neovascularization in experimental hind-limb ischemia. *Blood*. 2010;115(18):3843–3851.
21. Stalin J, Nollet M, Garigue P, et al. Targeting soluble CD146 with a neutralizing antibody inhibits vascularization, growth and survival of CD146-positive tumors. *Oncogene*. 2016;35(42):5489–5500.
22. Wang D, Duan H, Feng J, et al. Soluble CD146, a cerebrospinal fluid marker for neuroinflammation, promotes blood-brain barrier dysfunction. *Theranostics*. 2020;10:231–246.
23. Duan H, Luo Y, Hao H, et al. Soluble CD146 in cerebrospinal fluid of active multiple sclerosis. *Neuroscience*. 2013;235:16–26.
24. Bardin N, Blot-Chabaud M, Despoix N, et al. CD146 and its soluble form regulate monocyte transendothelial migration. *Arterioscler Thromb Vasc Biol*. 2009;29:746–753.
25. Duan H, Xing S, Luo Y, et al. Targeting endothelial CD146 attenuates neuroinflammation by limiting lymphocyte extravasation to the *CNS*. *Sci Rep*. 2013;3:1687.
26. Aiello LP, Avery RL, Arrigg PG, et al. Vascular endothelial growth factor in ocular fluid of patients with diabetic retinopathy and other retinal disorders. *N Engl J Med*. 1994;331(22):1480–1487.
27. Uzzan B, Nicolas P, Cucherat M, Perret GY. Microvessel density as a prognostic factor in women with breast cancer: a systematic review of the literature and meta-analysis. *Cancer Res*. 2004;64(9):2941–2955.
28. Meert AP, Paesmans M, Martin B, et al. The role of microvessel density on the survival of patients with lung cancer: a systematic review of the literature with meta-analysis. *Br J Cancer*. 2002;87(7):694–701.
29. Weidner N. Current pathologic methods for measuring intratumoral microvessel density within breast carcinoma and other solid tumors. *Breast Cancer Res Treat*. 1995;36(2):169–180.
30. Bringmann A, Pannicke T, Grosche J, et al. Müller cells in the healthy and diseased retina. *Prog Retin Eye Res*. 2006;25(4):397–424.
31. Jouve N, Bachelier R, Despoix N, et al. CD146 mediates VEGF-induced melanoma cell extravasation through FAK activation. *Int J Cancer*. 2015;137:50–60.
32. Neidhart M, Wehrli R, Brühlmann P, Michel BA, Gay RE, Gay S. Synovial fluid CD146 (MUC18), a marker for synovial membrane angiogenesis in rheumatoid arthritis. *Arthritis Rheum*. 1999;42:622–630.
33. Ito T, Tamura N, Okuda S, et al. elevated serum levels of soluble CD146 in patients with systemic sclerosis. *Clin Rheumatol*. 2017;36:119–124.
34. Miyamoto K, Khosrof S, Bursell SE, et al. Prevention of leukostasis and vascular leakage in streptozotocin-induced diabetic retinopathy via intercellular adhesion molecule-1 inhibition. *Proc. Natl. Acad. Sci. USA*. 1999;96:10836–10841.

Investigative Ophthalmology & Visual Science